Eur Biophys J (2010) 39:337–343
DOI 10.1007/s00249-009-0502-5

BIOPHYSICS LETTER

Lambda exonuclease digestion of CGG trinucleotide repeats

R. S. Conroy · A. P. Koretsky · J. Moreland

Received: 8 December 2008 / Revised: 28 April 2009 / Accepted: 7 June 2009 / Published online: 27 June 2009

Abstract Fragile X syndrome and other trinucleotide diseases are characterized by an elongation of a repeating DNA triplet. The ensemble-averaged lambda exonuclease digestion rate of different substrates, including one with an elongated FMR1 gene containing 120 CGG repeats, was measured using absorption and fluorescence spectroscopy. By use of magnetic tweezers sequence-dependent digestion rates and pausing was measured for individual lambda exonucleases. Within the triplet repeats a lower average and narrower distribution of rates and a higher frequency of pausing was observed.

Keywords Biophysics · Single molecule · Magnetic tweezers · Lambda exonuclease · Fragile X syndrome

Introduction

In the past two decades, at least 18 genetic neurodegenerative diseases have been linked with the expansion of repeating DNA triplets, resulting in disorders which include myotonic dystrophy, Huntington's disease, and Fragile X syndrome (Gatchel and Zoghbi 2005). DNA triplet repeats, for example $(CGG)_m$ or $(GAA)_m$ where $m = 4$–50, occur naturally throughout the genome, primarily in non-coding regions. Fragile X syndrome was the first identified, and is the most commonly studied, triplet repeat disease (Kremer et al. 1991). The original fragile site, FRAXA, is in the 5′ untranslated region of the FMR1 gene and the repeating CGG codon is subject to expansion from the normal range of 6–60 repeats to more than 200 repeats in the pathogenic state. Although these repeats have a B-DNA structure, their persistence length has been measured to be 60% less than that of random DNA (Bacolla et al. 1997). These repetitive sequences can also give rise to secondary structures, in particular hairpins, depending on DNA density, pH, ionic strength, and superhelical density (Usdin and Grabczyk 2000).

Both the causes and mechanisms by which the expansion of the triplet repeats occur are not resolved though a number of models have been proposed, including a number mediated by secondary structures (Wang and Vasquez 2006). Mechanistic evidence at the enzyme level has been aided by the observation of stalling of DNA polymerase in vitro (Mirkin and Mirkin 2007). Single-molecule assays observing the operation of individual enzymes and complexes and quantifying the influence of structure and environment may help further discriminate between the models.

Lambda exonuclease, a 24-kDa highly processive enzyme which hydrolyzes one strand of double-stranded DNA (dsDNA) in the 5′ to 3′ direction, has been studied previously in single-molecule experiments using pseudo-random DNA sequences. The average digestion rate has been measured to be 12 nt/s (Perkins et al. 2003), 15–20 nt/s (Dapprich 1999), and 32 nt/s (van Oijen et al. 2003) with an instantaneous rate varying between 0 and 100 nt/s. Sequence-dependence digestion rates (van Oijen et al. 2003) and pausing of up to 12 s correlating with DNA

R. S. Conroy (✉) · A. P. Koretsky
Laboratory of Functional and Molecular Imaging,
National Institute of Neurological Disorders and Stroke,
National Institutes of Health, Bethesda, MD 20892, USA
e-mail: conroyri@mail.nih.gov

R. S. Conroy · J. Moreland
National Institute of Standards and Technology,
325 Broadway, Boulder, CO 80305, USA

motifs (Perkins et al. 2003) have also been observed. These traits have also been observed with other exonucleases (Kropp et al. 1995). Exonuclease activity is important within the repeats, because of the observation that flap-specific endonuclease FEN-1 is necessary for the resolution of secondary structures in some of the triplet repeat expansion models (Singh et al. 2007).

In this report the characteristics of individual enzymes processing repetitive DNA sequences are described, specifically the measurement of lambda exonuclease digestion of 120 CGG triplet repeats in an elongated FMR1 gene. Repetitive DNA sequences are important because of their association with a number of functions such as regulation and reorganization of the genome (Richards and Sutherland 1996). Repeating motifs can also form stable hairpins which have been studied at the single-molecule level (Woodside et al. 2006), however, the interaction of DNA-modifying enzymes with these motifs is not well understood at the single-molecule level. Using magnetic tweezers we combine the advantages of optical tweezers (Perkins et al. 2003) and flow-stretching experiments (van Oijen et al. 2003), enabling multiple enzymes to be studied in parallel without heating concerns and with freedom to adjust flow rates independently of the applied force.

We hypothesized that the 120 repeats of the GC-rich triplet CGG in the elongated region are similar to the GGCG motifs previously reported to correlate with pausing (Perkins et al. 2003) and require more energy to separate (Woodside et al. 2006) and therefore may provide a significant barrier to lambda exonuclease activity. Lower average and instantaneous digest rates and a higher frequency of pausing were measured for the elongated regions, supporting this hypothesis.

Materials and methods

An elongated FMR1 gene containing 120 CGG repeats was ligated into a pGL3-basic vector (Promega, Madison, WI, USA) using the *Mlu*I and *Bgl*II restriction sites and replicated in *E. coli* under antibiotic selection. This plasmid is subsequently referred to as pGL-CGG120. Six colonies were isolated from a streaked plate and used to inoculate 5-mL tubes of liquid LB broth containing ampicillin. Care was taken to limit growth in a shaking incubator to a maximum of 10 h at 37°C to preserve replication fidelity. Plasmids were isolated and purified using a Miniprep kit (QIAprep; Qiagen, Valencia, CA, USA) and ethanol precipitation and quantified by absorption at 260 nm (A_{260}) and 280 nm (A_{280}).

The length of the elongated triplet repeat region was checked by double digest of the plasmid DNA with *Mlu*I/*Bgl*II, and compared on a 1% agarose gel with a GC-rich optimized PCR amplification (Roche Applied Science, Indianapolis, IN, USA) of the FMR1 gene insert and a pair of standard DNA ladders (O'Generuler; Fermentas, Glen Burnie, MD, USA). Well defined bands at approximately 550 base pairs (bp) were observed from four of the isolated colonies and these samples were used in the subsequent experiments.

Two commercially available double-stranded DNA sequences, the linear 48.5-kilobase pair (kbp) lambda phage and the circular phiX174 phage sequences (New England Biolabs, Ipswich, MA, USA) were used as pseudo-random DNA references. DNA samples were stored at 4°C for up to 4 days, or at −80°C for up to 12 months. The concentration of stock DNA was between 200 and 1,000 μg/mL with an A_{260}/A_{280} ratio between 1.8 and 2.2.

Absorption measurements were made in disposable ultraviolet-grade cuvettes (UVettes; Eppendorf, Westbury, NY, USA) containing 0.95 mL buffer allowed to come to equilibrium for a background measurement before 5 μg of DNA was added. Both the pGL-CGG120 plasmid and phiX174 phage sequence were linearized with their unique XhoI restriction sites to provide comparable digestion substrates. Stock lambda phage DNA was placed in a 55°C water bath for 15 min and rapidly cooled on ice to minimize re-circularization and concatenation of the cos ends. Subsequently lambda exonuclease (New England Biolabs) was added, a baseline acquired, and then the digestion was initiated with an infusion of Mg^{2+}. The rate was determined from curve fitting of the time course of measurements at 260 nm and 280 nm, which were recorded at 15-s intervals. The temperature-controlled stage of the spectrometer (Spectramax 384+; Molecular Devices, Sunnyvale, CA, USA) was set at 25°C, except for the temperature-dependent measurements with lambda phage DNA at 20, 30 and 37°C. Fitting to extract the digestion rate and analysis of the curves was carried out in Origin (OriginLab, Northampton, MA, USA). Statistical uncertainties are described by the standard deviation, and the significance level was set at $P < 0.05$.

Measurement of the digestion rate using fluorescence spectroscopy was carried out using a fluorescence spectrometer (Fluorolog FL3-22; Jobin Yvon, Edison, NY, USA). A 1:20,000 dilution of OliGreen (Invitrogen, Carlsbad, CA, USA), which has been reported to have a linear response for both dsDNA and ssDNA concentration (Bio-Tek 2001) was used to label 100 ng samples of dsDNA. Using a time course of excitation at 490 nm and measurement of emission at 520 nm at 1-s intervals, the resulting fluorescence decay curves were analyzed. Measurement rate was increased to 0.5-s intervals for the elongated FMR1 fluorescent digest, which was prepared from the replicated plasmid by a double digest (*Mlu*I/*Bgl*II) followed by purification on a 1.5% agarose gel (Qiaex II; Qiagen).

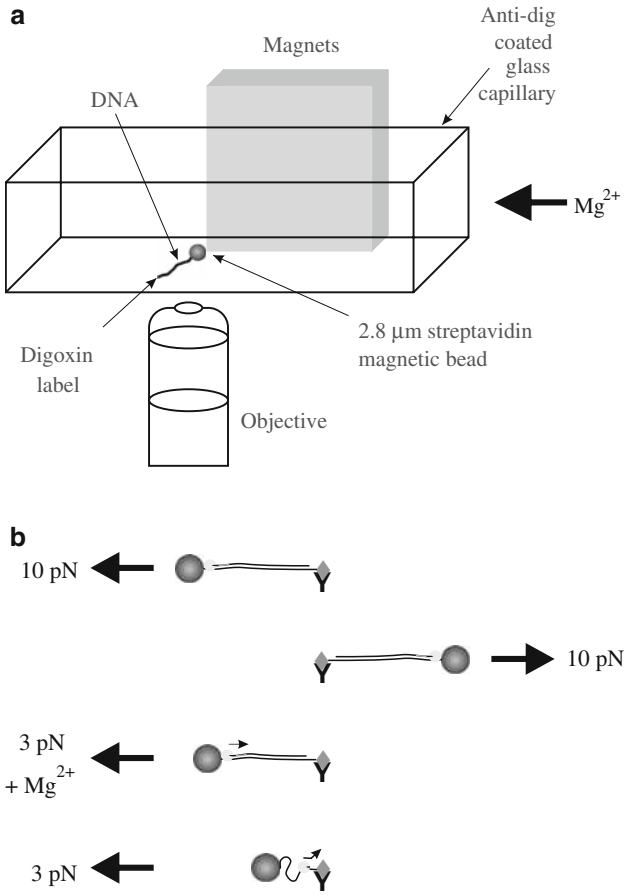

Fig. 1 **a** Schematic of the experimental setup used for the single-molecule experiments. One end of the DNA sequence is attached to the inner surface of a glass capillary by an antibody–antigen reaction and is stretched using a magnetic bead attached to the other end via a biotin–streptavidin reaction (not to scale). **b** After stretching the DNA in opposite directions with 10 pN to determine point of attachment and a single tether, the force was reduced to 3 pN and Mg^{2+} added to one end of the capillary. As the exonuclease digests one of the two strands, the persistence length and end-to-end distance decreases

A schematic of the setup used for the single-molecule experiments in shown in Fig. 1a. Following an approach similar to one previously described (Danilowicz et al. 2004), double digestion of the pGL-CGG120 plasmid with NcoI/XhoI provided two distinct overhangs on to which three oligos were ligated. One oligo included a digoxin label for attachment to the inner surface of a $1 \times 1 \times 10$ mm glass capillary (Vitrocells, Mountain Lakes, NJ, USA) previously incubated with anti-digoxin. Another oligo included a biotin label for attachment to a streptavidin labeled 2.8-µm diameter magnetic bead (Invitrogen) on the opposite end of the same DNA strand, making the other strand available for complete digestion by an exonuclease.

After diluting and washing 1-µL of the stock beads three times in an Mg^{2+}-free buffer suggested by the enzyme supplier, 10 attomoles of the modified linearized plasmid was incubated with the beads and lambda exonuclease enzyme for 15 min in a slow rotator. After magnetic separation and resuspension, approximately 100-µL of the suspension was loaded into the capillary using surface tension.

The experimental procedure for the single-molecule experiments is described in Fig. 1b. After 10 min of incubation, a stack of five 5-mm diameter neodymium, iron, boron permanent magnets (Master Magnetics, Castle Rock, CO, USA) were used to apply an average force of 10 pN to the beads and detach any non-specifically bound beads. The DNA-bound beads were then stretched in the opposite direction using a complementary set of magnets and the force–extension curve recorded, before a final recorded stretch in the first direction to determine the point of attachment and the number of DNA tethers. Screening for beads with a force–extension curve characteristic of a single tether and symmetric stretching, the force was reduced to a force of 3 pN and a video sequence recorded using an IX-71 microscope (Olympus, Center Vally, PA, USA) with a 40× objective and a 1.4 million pixel, 12-bit, ORCA-ER (Hamamatsu, Bridgewater, NJ, USA) monochromatic camera using brightfield whitelight. The bound exonucleases were activated using an infusion of $MgCl_2$ into one end of the capillary and a video recorded for 30 min. To convert the video sequence to position data, a 5×5 Laplacian of a Gaussian filter with kernel for $\sigma = 5$ pixels was applied and an ImageJ plugin used to track the center-of-mass of the beads (Sage et al. 2005). A correction was applied to this position data before the rates were determined because of the change in angle of the DNA with respect to the surface as the end-to-end length of the DNA changed. The standard deviation in the position of a fixed bead measured in this way over a 10 min period, comparable to the duration of the experiments, was 15 nm.

Results and discussion

To provide an ensemble-averaged measurement of the digestion rate of lambda exonuclease for comparison with the single-molecule experiments, the digestion of the DNA sequences was examined using absorption and fluorescence spectroscopy. Figure 2a illustrates the digestion rate measured for each of the three unmodified substrates at 25°C. No significant difference was measured between the digestion rates of the two shorter substrates, which are both similar in length to the average processivity of lambda exonuclease, however the rate is significantly lower for the lambda phage substrate which is nine times longer and significantly longer than the average processivity of a single enzyme. For the 48,502-bp long lambda phage sequence with 50% GC content the rate was 10.8 ± 1.4 nucleotides

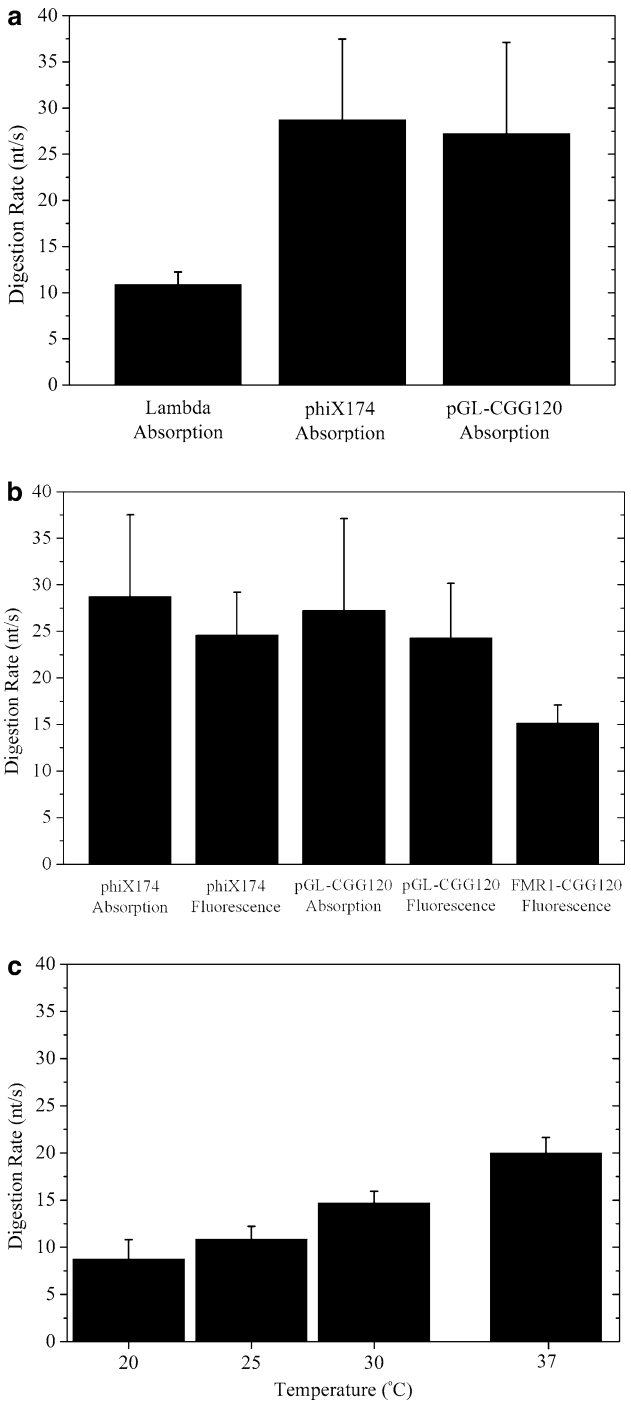

Fig. 2 Measurement of the lambda exonuclease digestion rate using spectroscopy. **a** Digestion rates at 25°C for the 48,502-bp lambda phage, 5,386-bp PhiX174 phage, and 5,373-bp pGL-CGG120 sequences measured by absorption. **b** Comparison of rates for the shorter sequences measured by absorption and fluorescence spectroscopy at 25°C. **c** Temperature-dependence of the digestion rate for the lambda phage sequence

per second (nt/s), for the 5,386-bp long phiX174 sequence with 44% GC content the rate was 28.7 ± 8.8 nt/s, and for the 5,373-bp long pGL-CGG120 sequence, with 52% GC content, the rate was 27.2 ± 9.9 nt/s. The rates measured using OliGreen as a fluorescent indicator, and illustrated in Fig. 2b, were not significantly lower at 24.6 ± 4.6 and 24.3 ± 5.9 nt/s, respectively. For the elongated FMR1 sequence, with 91% GC content, the rate measured by fluorescence was 15.1 ± 2.0 nt/s and significantly different from the overall pGL-CGG120 plasmid. Although DNA-sensitive dyes have been observed to inhibit exonuclease activity previously (Subramanian et al. 2003; Yakovleva et al. 2006), the related PicoGreen dye was found to cause the least perturbation when used to measured DNAase activity (Tolun and Myers 2003).

The temperature dependence of the digest rate of the lambda phage sequence was measured by absorption and the results shown in Fig. 2c. The average rate measured by absorption at 260 nm for the 48502-bp long lambda phage sequence was 10.8 ± 1.4 nt/s at 25°C. This rate increased to 14.7 nt/s at 30°C and 20.0 nt/s at 37°C. These rates are consistent with previous measurements (Carter and Radding 1971; Perkins et al. 2003) and indicate that small temperature fluctuations do not significantly affect digestion rate at room temperature. At more extreme temperatures, the underlying temperature–force phase diagram for DNA is more complicated (Danilowicz et al. 2004) and may contribute to more significant variations. At 37°C the rate is higher than that previously reported for fluorescently labeled DNA (Subramanian et al. 2003) although no account was taken here in the analysis for the possibility of increased ssDNA activity of lambda exonuclease at higher temperatures (Little 1981).

With biotin and digoxin-labeled oligos ligated on to both ends of all three sequences, the digestion rate of the lambda phage sequence measured by absorption decreased to 5.2 ± 3.1 nt/s, 12.4 ± 5.6 nt/s for the pGL-CGG120, sequence and 12.7 ± 4.8 nt/s for the phiX174 sequence. These results are consistent with the expectation that only one enzyme is active on the substrate, working on only one of the two strands.

Although a significant difference in the digestion rate was measured for the GC-rich elongated FMR1 gene, the data were collected from ensemble averaging of at least one billion digestions and do not indicate whether the decrease is because of pausing or slower procession through the GC-rich sequence.

Complementing the ensemble measurements, magnetic tweezers were used to stretch individual pGL-CGG120 DNA sequences in the image plane of a microscope and the decrease in persistence length between dsDNA and ssDNA used as readout of the digestion rate (Dapprich 1999; Matsuura et al. 2001; Perkins et al. 2003; van Oijen et al. 2003). In a single field-of-view, the maximum number of digestions observed to go to completion was limited to three. This reflected the need to keep the density of DNA-labeled

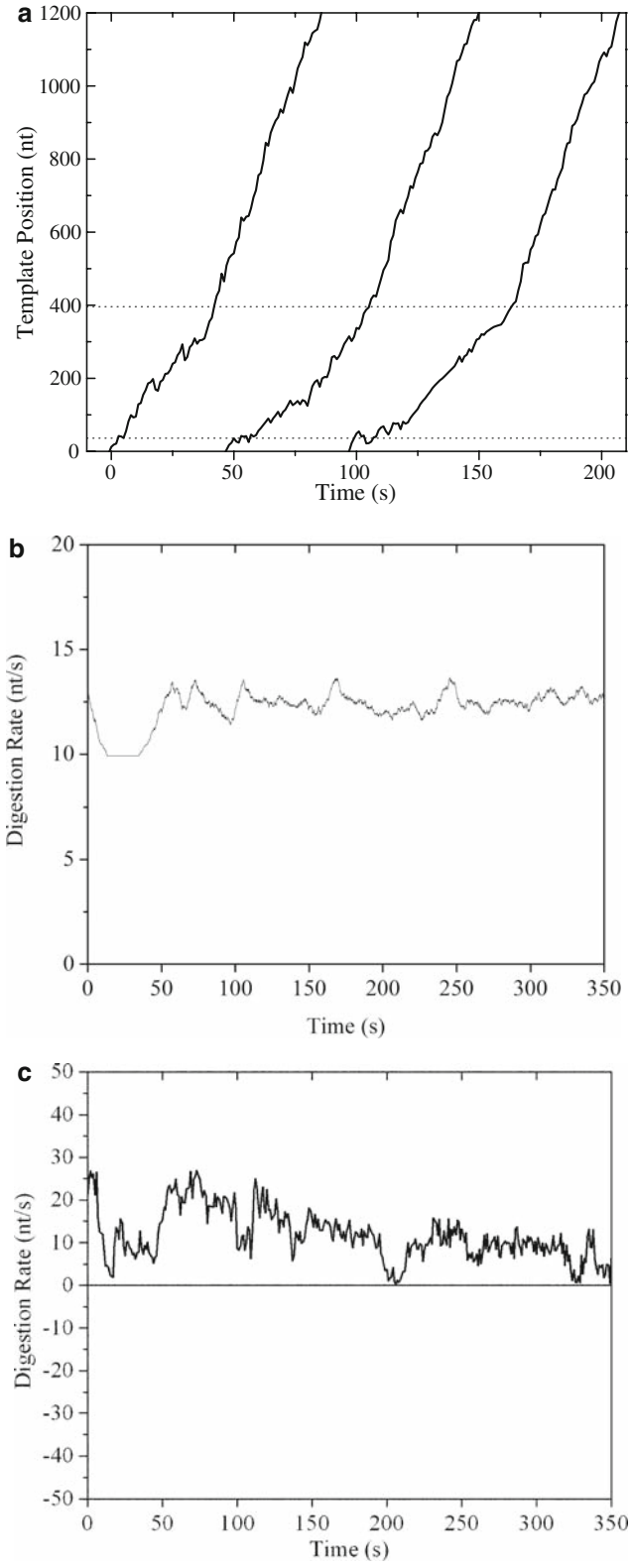

◀ **Fig. 3** Data from individual lambda exonuclease digests of the pGL-CGG120 sequence. **a** Partial traces of template position versus time for three independent digestions (offset by 50-s intervals, smoothed with a 10 s moving average and truncated at 1,200 bp for clarity). The area between the *dotted lines* represents the region of the CGG repeats in the template. **b** Simulation of the digestion rate based on bond energies for the complete pGL-CGG120 sequence using a 100-bp moving average. **c** Digestion rate calculated from the center trace of **a** smoothed with a 10-s moving average

beads low to avoid aggregation, the low DNA concentration used to give one tether per bead, and that less than 10% of the beads observed with force–extension curves characteristic of a single tether went to completion, primarily because of bead–DNA–surface interactions characterized by a significant change in the motion of the bead.

Figure 3a illustrates the partial trajectories of three digestions which went to completion. It has previously been observed that the digestion rate of lambda exonuclease is sequence-specific, because of the energy landscape associated with the Gibb's free energy calculated from the energy required to melt the hydrogen bonds between base pairs and the stacking energy of the helix (van Oijen et al. 2003). Figure 3b is a prediction of the digestion rate based on the Gibb's free energy of the pGL-CGG120 sequence, based on an average rate of 12.4 nt/s measured by absorption spectroscopy. Figure 3c is a plot of the experimentally measured rate from a single digestion, with a 10 s moving average used to smooth the data. For the complete pGL-CGG120 sequence, the Pearson product–moment correlation coefficient of individual complete digestions with the predicted rate was $r^2 = 0.184 \pm 0.088$ ($n = 10$), indicating a weak correlation between the digestion rate and the Gibb's free energy landscape derived from the sequence information. Within the region of the triplet repeats near the beginning of the digestions the correlation coefficient was $r^2 = 0.61 \pm 0.12$. When the digestion sequences were averaged first and then the correlation coefficient calculated, $r^2 = 0.24$ for the complete sequence and $r^2 = 0.68$ for the region of the triplet repeats, indicating the smoothing of noise and variation in enzyme activity increases correlation. It should be noted that the model used to correct for the angle of the DNA in these experiments does not remove all trends (as can be seen from Fig. 3c) and the sequences not optimally aligned, which may also lead to underestimation of the correlation.

The rate statistics from the ten complete digestions are plotted in Fig. 4a smoothed using a three-second moving average, to illustrate the spread in "instantaneous" enzyme digestion rate. From a Gaussian fit of all the data from the ten digests ($R^2 = 0.975$) displayed in Fig. 4a this smoothed "instantaneous" rate of an individual enzyme in a one-second time interval was 14.7 ± 26.3 nt/s. This result is within the statistical error of the ensemble absorption measurements under the same conditions and is in good agreement with previous measurements of mean rate and distribution. From the ten digests, the "instantaneous" digestion rate in the region of the triplet repeats is illustrated in Fig. 4b with

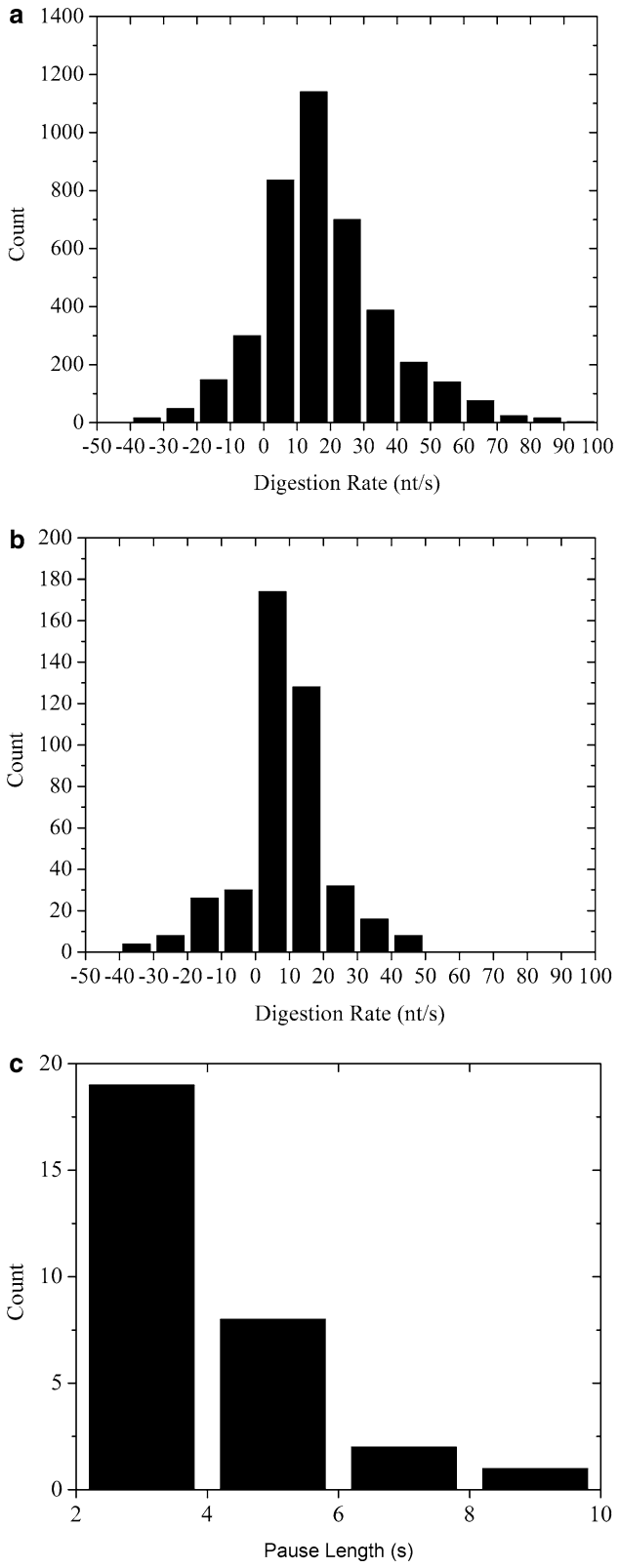

◀ **Fig. 4** Digestion rate statistics from a set ($n = 10$) of smoothed (3-s moving average) one-second "instantaneous" rates of individual lambda exonuclease digestions of the pGL-CGG120 sequence. Distribution of rates for **a** the complete pGL-CGG120 sequence and **b** the CGG repeat region. **c** Within the triplet repeat region the distribution of pause times, for which the measured digestion rate was not significantly different from 0 nt/s for more than 2 s

a fitted average of 8.6 ± 13.5 nt/s, and is statistically significantly different from a random sample of the same size taken from the pooled population data, but consistent with the expectation for half of the rate measured for the fluorescent digest of the elongated FMR1 sequence. The lower average and narrower distribution of "instantaneous" digestion rates within the triplet repeat sequence supports our hypothesis of the GC-rich region providing a significant barrier for lambda exonuclease activity.

A definition was used to define pause points, where the "instantaneous" digestion rate was consecutively below 10 nt/s for at least 2 s, and an independent two-sample *t* test of the rates within the pause point was not statistically significantly different from 0 nt/s. The distribution of the length of these pauses within the triplet repeat region is illustrated in Fig. 4c. Although the distribution of pause times is similar to those previously reported to correlate with motifs containing GGCG (Perkins et al. 2003) and observed both within the triplet repeats and in the surrounding vector sequence, no common pause points could be defined. The frequency of pausing in the region of the triplet repeats was 8.3 kbp^{-1} whereas the frequency of pausing in the rest of the sequence was 1.2 kbp^{-1}, although there was no significant difference in distribution of pause times between the two regions. This result supports the hypothesis that GC-rich repetitive sequences provide a significant barrier to lambda exonuclease activity by increasing the probability of pausing in addition to reducing the average digestion rate.

Conclusions

We have measured a sequence-dependent rate and pausing of individual lambda exonuclease enzymes during the digestion of a DNA sequence containing 120 CGG repeats. A decrease in digestion rate was resolved using fluorescence spectroscopy and confirmed by the observation of individual enzymes, which showed the decrease was due to a combination of a narrower distribution of "instantaneous" rates within the elongated repeating sequence and an increase in pause frequency.

It should be noted that these results were biased by the requirements for the force-extension of the tether to be characteristic of a single B-conformation dsDNA molecule and for the digestion to have gone to completion, limiting analysis to only temporary pauses in characteristic single dsDNA tethers. Results from absorption spectroscopy indicated that at least 75% of double-stranded base pairs were

converted to single-stranded base pairs at an average rate within the experimental error of the single-molecule experiments, indicating that these assumptions did not significantly bias the average of the single-molecule results.

Magnetic tweezers have the advantages of not dissipating energy, parallel data collection, and not requiring continuous flow, providing a strong platform for further study of enzyme interaction with repetitive DNA structures. Work is in progress to observe the re-creation of the complementary strand by DNA polymerase, following digestion by lambda exonuclease, with the objective of characterizing replication fork stalling of individual complexes. A comparison of sequences containing repeats considered to be within the normal range with pre and full mutation sequences taking into account epigenetic differences would give a more fine-grained analysis of the mechanisms which give rise to expansion. These techniques can also be applied to other trinucleotide repeat disorders, for example Fredreich's ataxia, which do not have the same GC-rich characteristics as Fragile X syndrome.

Acknowledgments RC acknowledge the support of a National Research Council Research Associateship Award and the help of Karen Usdin and Daman Kumari of NIDDK who supplied the elongated FMR1 sequence and helped with preparation, replication and isolation of the plasmid, and Keir Neuman for critical feedback. This research was supported in part by the Intramural Research Program of the NINDS, NIH.

References

Bacolla A, Gellibolian R, Shimizu M, Amirhaeri S, Kang S, Ohshima K, Larson JE, Harvey SC, Stollar BD, Wells RD (1997) Flexible DNA: genetically unstable CTG center dot CAG and CGG center dot CCG from human hereditary neuromuscular disease genes. J Biol Chem 272:16783–16792

BioTek (2001) Quantitation of ssDNA using OliGreen fluorescent stain. In: Budowle B (ed) Application notes. BioTek Inc., Winooski, VT. http://www.biotek.com/resources/docs/FL600_Quantitation_using_OliGreen.pdf

Carter DM, Radding CM (1971) The role of exonuclease and beta protein of phage lambda in genetic recombination. II. Substrate specificity and the mode of action of lambda exonuclease. J Biol Chem 246:2502–2512

Danilowicz C, Kafri Y, Conroy RS, Coljee VW, Weeks J, Prentiss M (2004) Measurement of the phase diagram of DNA unzipping in the temperature–force plane. Phys Rev Lett 93:078101

Dapprich J (1999) Single-molecule DNA digestion by lambda-exonuclease. Cytometry 36:163–168

Gatchel JR, Zoghbi HY (2005) Diseases of unstable repeat expansion: mechanisms and common principles. Nat Rev Genet 6:743–755

Kremer EJ, Pritchard M, Lynch M, Yu S, Holman K, Baker E, Warren ST, Schlessinger D, Sutherland GR, Richards RI (1991) Mapping of DNA instability at the fragile X to a trinucleotide repeat sequence p(CCG)n. Science 252:1711–1714

Kropp B, Leoni L, Sampaolese B, Savino M (1995) Influence of DNA superstructural features and histone amino-terminal domains on nucleosome positioning. FEBS Lett 364:17–22

Little JW (1981) Lambda exonuclease. Gene Amplif Anal 2:135–145

Matsuura S, Komatsu J, Hirano K, Yasuda H, Takashima K, Katsura S, Mizuno A (2001) Real-time observation of a single DNA digestion by lambda exonuclease under a fluorescence microscope field. Nucleic Acids Res 29:E79

Mirkin EV, Mirkin SM (2007) Replication fork stalling at natural impediments. Microbiol Mol Biol Rev 71:13–35

Perkins TT, Dalal RV, Mitsis PG, Block SM (2003) Sequence-dependent pausing of single lambda exonuclease molecules. Science 301:1914–1918

Richards RI, Sutherland GR (1996) Repeat offenders: simple repeat sequences and Y genetic problems. Hum Mutat 8:1–7

Sage D, Neumann FR, Hediger F, Gasser SM, Unser M (2005) Automatic tracking of individual fluorescence particles: application to the study of chromosome dynamics. IEEE Trans Image Process 14:1372–1383

Singh P, Zheng L, Chavez V, Qiu JZ, Shen BH (2007) Concerted action of exonuclease and gap-dependent endonuclease activities of FEN-1 contributes to the resolution of triplet repeat sequences (CTG)(n)- and (GAA)(n)-derived secondary structures formed during maturation of Okazaki fragments. J Biol Chem 282:3465–3477

Subramanian K, Rutvisuttinunt W, Scott W, Myers RS (2003) The enzymatic basis of processivity in lambda exonuclease. Nucleic Acids Res 31:1585–1596

Tolun G, Myers RS (2003) A real-time DNase assay (ReDA) based on PicoGreen fluorescence. Nucleic Acids Res 31:e111

Usdin K, Grabczyk E (2000) DNA repeat expansions and human disease. Cell Mol Life Sci 57:914–931

van Oijen AM, Blainey PC, Crampton DJ, Richardson CC, Ellenberger T, Xie XS (2003) Single-molecule kinetics of lambda exonuclease reveal base dependence and dynamic disorder. Science 301:1235–1238

Wang GL, Vasquez KM (2006) Non-B DNA structure-induced genetic instability. Mutat Res Fundam Mol Mech Mutagen 598:103–119

Woodside MT, Behnke-Parks WM, Larizadeh K, Travers K, Herschlag D, Block SM (2006) Nanomechanical measurements of the sequence-dependent folding landscapes of single nucleic acid hairpins. Proc Natl Acad Sci USA 103:6190–6195

Yakovleva L, Handy CJ, Yagi H, Sayer JM, Jerina DM, Shuman S (2006) Intercalating polycyclic aromatic hydrocarbon-DNA adducts poison DNA relegation by Vaccinia topoisomerase and act as roadblocks to digestion by exonuclease III. Biochemistry 45:7644–7653